Journal of Applied Polymer Science

Production of Polyamic Acid in Supercritical Carbon Dioxide with *N,N*-Dimethylformamide

Masashi Haruki, Yumi Hasegawa, Naoya Fukui, Shin-ichi Kihara, Shigeki Takishima
Department of Chemical Engineering, Graduate School of Engineering, Hiroshima University, 1-4-1 Kagamiyama, Higashi-Hiroshima 739-8527, Japan
Correspondence to: M. Haruki (E-mail: mharuki@hiroshima-u.ac.jp)

ABSTRACT: To develop a microscale processing technique for aromatic polyimides (APIs) in supercritical carbon dioxide ($scCO_2$), the relationships between the polymerization condition, the phase behavior during polymerization and the molecular weight of polyamic acid (PAA)—an intermediate in the production of polyimides—were investigated in $scCO_2$ at 50°C. 4,4′-Diaminodiphenyl ether (ODA) and pyromellitic dianhydride (PMDA) were used as monomers of aromatic diamine and tetracarboxylic dianhydride, respectively, and 19 mol % of N,N-Dimethylformamide (DMF) was added to $scCO_2$ as a cosolvent. The cloudy phase appeared immediately when ODA and PMDA were mixed under any experimental conditions. However, the appearances of the phase behaviors during polymerization differed depending on the polymerization pressure and the initial monomer concentration. The number average molecular weight of PAA increased as the monomer concentration was increased in $scCO_2$, as was the case with polymerization in pure DMF at atmospheric pressure, despite differences in the phase behavior. On the other hand, the weight average molecular weight of PAA depended on the phase behaviors during polymerization along with the monomer concentration. Moreover, API obtained from the PAA synthesized in $scCO_2$ was analyzed using a Fourier transform infrared spectrophotometer and thermogravimetric analyzer, and the results were compared with those of APIs obtained by the solution polymerization. © 2013 Wiley Periodicals, Inc. J. Appl. Polym. Sci. **2014**, *131*, 39878.

KEYWORDS: polyimides; phase behavior; polycondensation; synthesis and processing

Received 28 February 2013; accepted 19 August 2013
DOI: 10.1002/app.39878

INTRODUCTION

Aromatic polyimide (API) is one of the most representative of engineering plastics, and is distinguished by its mechanical strength and heat resistance. Moreover, API is also known as an excellent electrical insulation material because of its quite low dielectric constant. Therefore, API has been used in a variety of industrial fields, from electronics to aerospace.[1–6] There are mainly two ways to produce API industrially: solution polymerization and vapor deposition polymerization (VDP). In solution polymerization, API is produced via a two-step method using a liquid solvent, as shown in Figure 1. In the first step, polyamic acid (PAA) is synthesized from equivalent molars of aromatic diamine and tetracarboxylic dianhydride in an aprotic polar solvent at a relatively low temperature. Then, API is produced by the dehydration reaction of PAA using thermal action or a dehydration agent in the second step. To obtain the desired shapes of molding products, a PAA solution is formed into desired shapes before imidization because the high mechanical strength and high thermal stability of API make it quite difficult to be shaped into an objective form. For example, API thin film is formed on a wafer by coating with a PAA solution, followed by baking to obtain API. Moreover, microparticles of API have been recently produced using precipitation polymerization to obtain engineering plastic microparticles. Asao et al.[7] investigated the relationships between reaction solvent species and the particle size of PAA to obtain functional API particles. However, the PAA solution has high viscosity, and it is difficult to penetrate the insides of the microscopic spaces. Therefore, this technique seems to be inadequate for processing inside the microscopic spaces.

As for the VDP process, both monomers are vaporized in each reservoir at high temperature, and then they are supplied on the surface of the materials, which are highly heated to produce API films or layers. The VDP has many advantages: non-solvent residue within the film, a reduction in environmental health problems, and the ability to supply the monomers into deep portions of a microscopic space compared with the solution polymerization. The VDP was first reported by Iijima et al.[8,9] and Salem et al.[10] in the 1980s. Recently, the VDP was also used to heal flaws on the surface of carbon fiber with API by

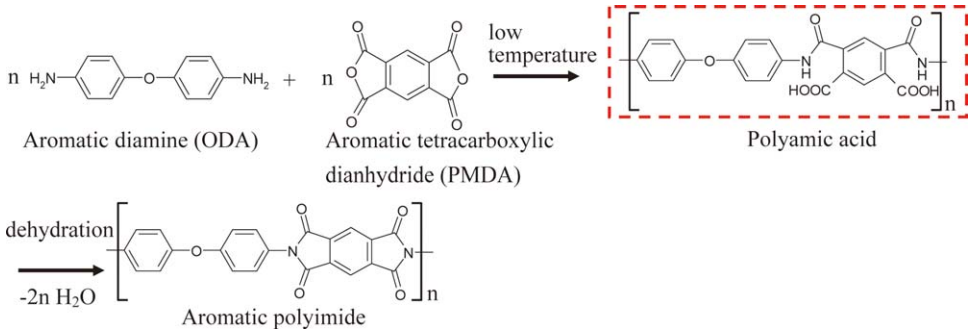

Figure 1. Scheme for the synthesis of API (2-step method). [Color figure can be viewed in the online issue, which is available at wileyonlinelibrary.com.]

Naganuma et al.,[5] and the filament tensile properties of API coating have been improved significantly. However, the production rate of APIs via VDP often depends on the vapor or sublimation pressures of the monomers, although most API monomers show quite low values. Therefore, the producible thickness of the film and the fillable volume of the space are limited.

Recently, electronic instruments including semiconductor devices have become smaller and more complicated in shape, and the techniques of API microfabrication are now required, such as filling API into a microscopic space. For example, the method integrating many substrates has received much attention to satisfy the demands from the viewpoints of both functional advancement and downsizing of the electric instruments.[11–13] To stack substrates, the clearances between the layers of the substrates must be narrowed and each substrate must connect using many bump electrodes. Therefore, the clearances become quite complicated microscopic spaces where API should be filled as an insulator and a reinforcement material. In this situation, supercritical carbon dioxide ($scCO_2$) has the potential to be a promising solvent because transport physical properties of $scCO_2$ such as diffusivity and viscosity are favorable to penetrate into microscopic space, and the amount of the organic substance in $scCO_2$ can be much higher than that obtained by vaporization of the substance. Namely, $scCO_2$ can deliver a great amount of API monomers and PAA into the deep portions of a microscopic space where reactions to API occur. With respect to the processing of metal complexes to fill metal compounds into microscopic spaces, many advantages of the microfabrication technique using $scCO_2$ have been reported.[14–16] On the other hand, polymers with a high molecular weight could not dissolve in $scCO_2$ except for a few kinds of polymers such as fluorinated polymers and siloxane polymers,[17] therefore, only low molecular weight PAA dissolved in $scCO_2$ and small PAA precipitates that disperse well in $scCO_2$ can be delivered in microscopic space as well as the monomers. Thus, a fundamental knowledge of the polymerization of API monomers, such as phase behavior during polymerization, is necessary to effectively deliver PAA and monomers into microscopic spaces and to design the entire process because the physical properties of $scCO_2$ are dramatically changed by temperature and pressure.

As for the polymerization in $scCO_2$, radical polymerization using vinyl monomers have been well studied in order to produce polymer particles by dispersion polymerization, which includes controlled/living radical polymerization.[18–20] On the other hand, the number of studies that have focused on step-growth polymerizations in $scCO_2$ is quite small compared with the focus on radical polymerization.[18,21] As for polyimides, Said-Galiyev et al.[22] succeeded in first producing API with fluorinated functional groups in $scCO_2$ in 2003, however, there have been no further reports since the first study. Therefore, a sufficient amount of experimental data and knowledge have yet to be accumulated for the development of new methods of processing for the microfabrication of API using $scCO_2$.

In our previous study,[23,24] first the solubilities of 4,4′-diaminodiphenyl ether (ODA) and pyromellitic dianhydride (PMDA), which are representative monomers of aromatic diamine and tetracarboxylic dianhydride, respectively, in $scCO_2$ were measured. Moreover, the cosolvent effect of *N,N*-dimethylformamide (DMF) and acetone on the solubilities of both monomers were investigated at the range of the cosolvent concentration up to approximately 20 mol %. As a result, DMF showed a higher cosolvent effect compared with acetone, and the addition of even 10 mol % of DMF into $scCO_2$ raised the solubility of ODA and PMDA by about 50 and 100%, respectively, at 50°C and 20 MPa. In this study, the relationships between the polymerization condition, the phase behavior during polymerization reaction and the molecular weight of PAA were investigated to obtain fundamental knowledge of API production in $scCO_2$. Moreover, API obtained from the PAA synthesized in $scCO_2$ was analyzed using a Fourier transform infrared (FT-IR) spectrophotometer and thermogravimetric analyzer (TGA) in order to investigate the chemical structure and thermal stability of API obtained by the processing in $scCO_2$. ODA and PMDA were also used as monomers, and DMF was added to $scCO_2$ as a cosolvent as well as in the previous work.

EXPERIMENTAL

Materials

ODA with purity >99 wt % was purchased from Wako Pure Chemical Industries Co., and PMDA with a purity >97 mol % was purchased from Sigma-Aldrich Co. The chemical structures of both monomers are described in the reaction formula of

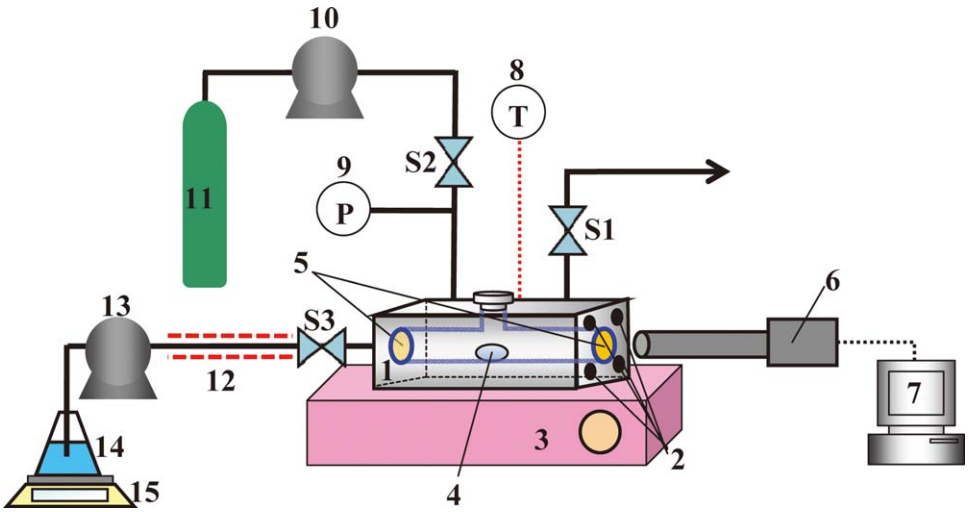

Figure 2. Schematic diagram of the experimental apparatus for polymerization in $scCO_2$. 1: high-pressure cell; 2: cartridge heaters; 3: ceramic hot stirrer; 4: Teflon-coated stirring bar; 5: Pyrex windows; 6: borescope with CCD camera; 7: personal computer; 8: thermocouple and temperature indicator; 9: pressure gauge and indicator; 10: HPLC pump for CO_2; 11: CO_2 cylinder; 12: line heater; 13: HPLC pump for DMF + PMDA solution; 14: DMF + PMDA solution in a glass flask; 15: electric balance; S1–S3: stop valves. [Color figure can be viewed in the online issue, which is available at wileyonlinelibrary.com.]

Figure 1, and they were solid materials at room temperature. CO_2 with a purity >99.5 vol % was purchased from Chugoku Sanso Co. Potassium bromide (KBr) with a purity >99.0 wt % was used for the FT-IR spectrophotometry and also was purchased from Wako Pure Chemical Industries Co. These chemicals were used without further purification. Moreover, DMF with a purity >99.7 vol %, which was used as a cosolvent added to $scCO_2$ and a moving bed for gel permeation chromatography (GPC), was purchased from Nacalai Tesque Co. DMF was dehydrated by molecular sieves before use.

Apparatus and Procedure for Polymerization in $scCO_2$

A batch-type apparatus equipped with CO_2 and monomer introduction portions was developed in this study to carry out the polymerization of ODA and PMDA in $scCO_2$. The schematic diagram of the apparatus is illustrated in Figure 2. During polymerization, a high-pressure cell (Toyokoatsu Co., 10 mm in internal diameter) with Pyrex windows at both ends was heated to the experimental temperature using four cartridge heaters. The temperature in the cell was measured by a thermocouple (Just Co., TSK type thermometer) connected with an indicator (Shimaden Co., SR94), and the uncertainty of the temperature measurement was estimated to within ±1°C. The precise internal volume of the cell (16.4 cm^3, subtracting the volume of a stirring bar) was determined using the pressure–volume–temperature relationship of nitrogen gas. Then a certain amount of the DMF + ODA solution, in which the concentration of ODA was previously determined, was introduced into the cell, and the amount of the solution introduced was measured using an electric balance (Mettler Toledo Co., AG204, uncertainty of ±0.1 mg). The solution was well agitated by a Teflon-coated stirring bar with a ceramic hot stirrer (As one Co., CHPS-250DN). Pure CO_2 was introduced using an HPLC pump (Jasco Co., PU-2080-CO_2 Plus), and the amount of CO_2 in the cell was estimated by the volume of mixing data for the CO_2 + DMF system[25]. Namely, the amount of CO_2 was determined by the amount of DMF in the cell and pressure after CO_2 introduction. The pressure of the system was measured using a pressure transmitter (Huba Control Co., Type-680, uncertainty of ±0.005 MPa) connected to a digital indicator (Axis Co., GR3666). In this stage, a homogeneous phase was obtained for the CO_2 + DMF + ODA mixture, although the pressure in the cell did not reach the experimental level. Finally, PMDA dissolved in DMF was added to the cell via another HPLC pump (Jasco Co., PU-2080 Plus), and polymerization was initiated. The amount of the PMDA + DMF solution added was determined by another electric balance (As one Co., ASP602F, uncertainty of ±10 mg). From the reaction formula shown in Figure 1 and in the literature,[26] the molar numbers of ODA and PMDA used for polymerization should be the same in order to obtain PAA with high molecular weight. However, our preliminary investigation of the polymerization in pure DMF indicated that adding slightly more of molar number of PMDA than that of ODA was better. This might be caused by the deactivation of a little of PMDA during preparation of the polymerization reaction. Therefore, about 1.1–1.2 of the molar ratio of PMDA to ODA was adopted throughout this study. The phase behavior inside the cell was observed using a borescope (Olympus Co., R100 series) with a CCD camera (Sanyo Co., VCC D473) system. After the polymerization was finished, CO_2 was discharged and the PAA that had dissolved in DMF of a cosolvent was collected. The polymerizations for each condition were carried out at least twice.

Condition of the GPC for Molecular Weight Analysis

The average molecular weight and molecular weight distribution (MWD) were determined by the GPC system with a differential refractive index detector (Shimadzu Co., RID-10A). Serially concatenated columns, Shodex KD-803 (Showa Denko K. K., exclusion limit of 7×10^4 g mol^{-1}) and Shodex KD-805

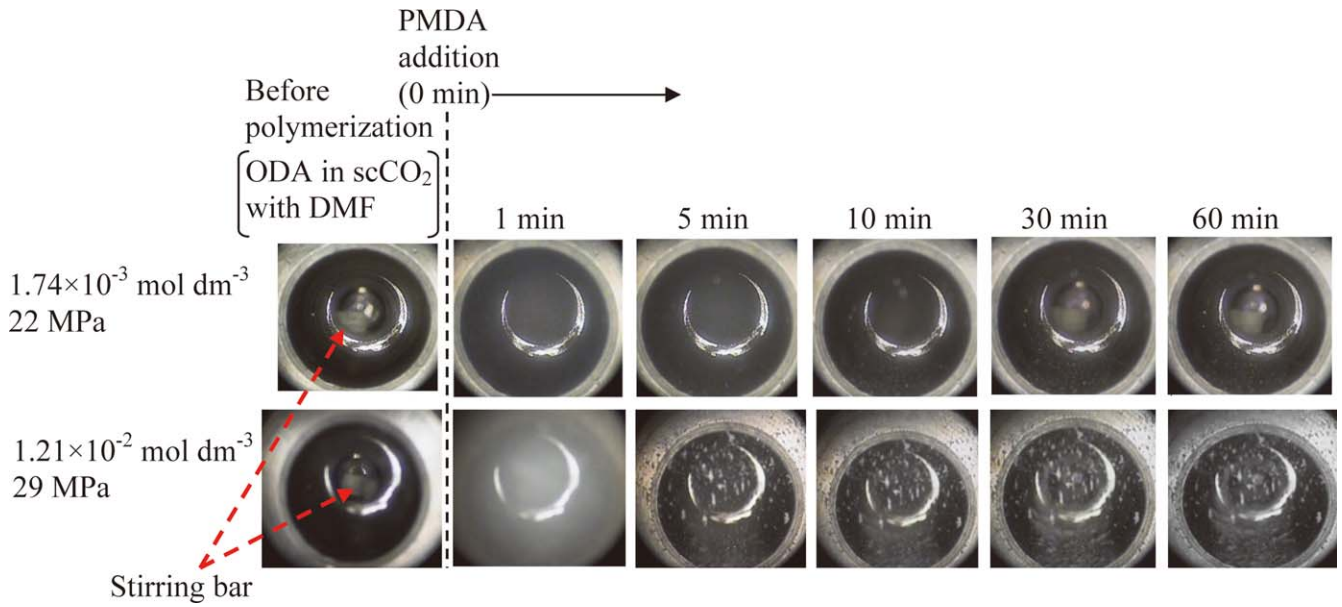

Figure 3. Images of the chronological changes in phase behaviors during polymerization for ODA concentrations of 1.74×10^{-3} mol dm^{-3} at 22 MPa and 1.21×10^{-2} mol dm^{-3} at 29 MPa. [Color figure can be viewed in the online issue, which is available at wileyonlinelibrary.com.]

(Showa Denko K. K., exclusion limit of 4×10^6 g mol^{-1}), were used for the GPC analysis, and the temperature of the column oven was set to 40°C. To use GPC analysis for PAA, the intramolecular interaction force caused by the carboxylic acid functional groups of PAA should be prevented.[27] Therefore, 15 mmol L^{-1} of lithium bromide and phosphoric acid were added to DMF of the moving bed. The flow rate of the eluent was set to 1.0 mL min^{-1}. Several molecular weights of standard polyethylene glycols (Agilent technologies Co.) and polyethylene oxides (Tosoh Co.) were used for preparation of the calibration curve. Thus, the molecular weights of PAA described in following sections are based on polyethylene glycol and polyethylene oxide.

Preparation of API for the FT-IR Spectrophotometry and TG Analysis

PAAs synthesized in $scCO_2$ with DMF, and in pure DMF, were imidized before the FT-IR spectrophotometry and TG analyses to avoid imidization during the analysis. In the imidization process, at first, the PAA solutions (PAA dissolved in DMF) were put on the silicon wafer which was heated up to 200°C by a hot plate to evaporate DMF. Then the residues on the wafer were cured at 250°C in air atmosphere for 24 or 48 h to obtain APIs by the thermostatic air bath. The APIs were analyzed using a FT-IR spectrophotometer (Shimadzu Co., IRPrestige-21) with the KBr pellet method, and by a thermogravimetric analyzer (Shimadzu Co., TGA 50) in air atmosphere.

RESULTS AND DISCUSSION

All polymerizations of ODA and PMDA were carried out in $scCO_2$ with DMF at 50°C because PAA should be prevented from changing into API during polymerization, and the solubilities of ODA and PMDA in $scCO_2$ with DMF were well clarified at 50°C in our previous work.[23] As for the concentration of DMF in $scCO_2$, 19 mol % was used for all polymerization, because according to the literature,[28] the $scCO_2$ + DMF mixture shows the homogeneous phase at any composition of DMF at more than about 10 MPa at 50°C, and approximately 20 mol % was considered to be an appropriate DMF concentration based on the results of the previous work. Namely, those values can produce a homogeneous phase of the CO_2 + DMF mixture with sufficient solubilities for both monomers. Moreover, it was also considered that the advantages of $scCO_2$ processing should be maintained—high diffusivity and low surface tension. In the polymerization, the concentrations of the monomers were prepared sufficiently lower than their saturated solubilities in the $scCO_2$ + DMF mixture under the same conditions in order to ensure the rapid dissolution of the monomers in $scCO_2$ and to avoid precipitation of the monomers during polymerization. The reaction time was set to 60 min based on the results of our preliminary experiments of polymerization in pure DMF. The chronological changes of phase behaviors during polymerization for the conditions of ODA concentration of 1.74×10^{-3} mol dm^{-3} at 22 MPa and 1.21×10^{-2} mol dm^{-3} at 29 MPa, which were the lowest and highest ODA concentrations in the present study, respectively, are shown in Figure 3. The transparent phases changed to cloudy phases immediately after PMDA was introduced into the cell regardless of the monomer concentration, as shown in the images, because $scCO_2$ is a relatively poor solvent for PAA obtained from ODA and PMDA under these conditions unlike such as fluorinated polymers, as described above. As the reaction progressed, PAA aggregates were precipitated at the bottom of the cell or onto the surface of the Pyrex windows, although the size of the aggregates seemed to depend on the monomer concentration. Finally, the cloudy phases of both ODA concentrations were returned to approximately the transparent phases because most of the PAA aggregates had precipitated, which was confirmed by the reappearance of the stirring bar inside the cell.

The MWDs of PAA obtained by the GPC analyses are described in Figure 4, and the relationships between the polymerization conditions and the number average molecular weight ($\overline{M}_n$) and

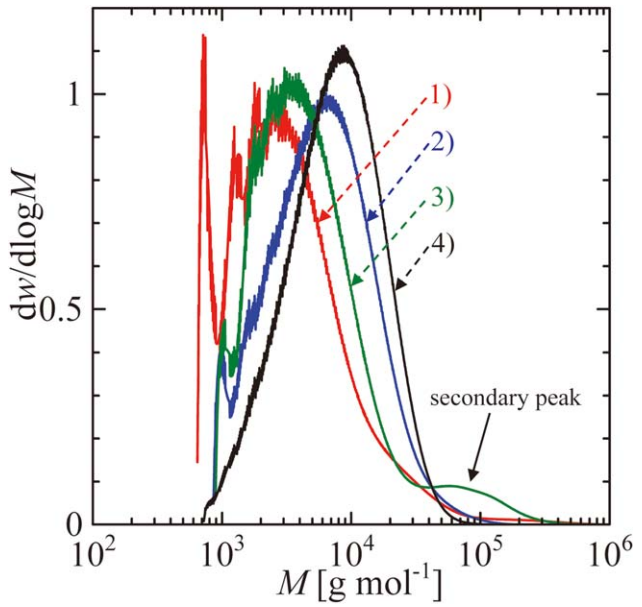

Figure 4. Molecular weight distributions of PAA polymerized in $scCO_2$ with 19 mol % DMF at 50°C and 60 min. ODA concentration and pressure for numbers of (1)–(4) are as follows: (1) 1.74×10^{-3} mol dm^{-3} and 22 MPa; (2) 6.01×10^{-3} mol dm^{-3} and 22 MPa; (3) 5.98×10^{-3} mol dm^{-3} and 30 MPa; (4) 1.21×10^{-2} mol dm^{-3} and 29 MPa. [Color figure can be viewed in the online issue, which is available at wileyonlinelibrary.com.]

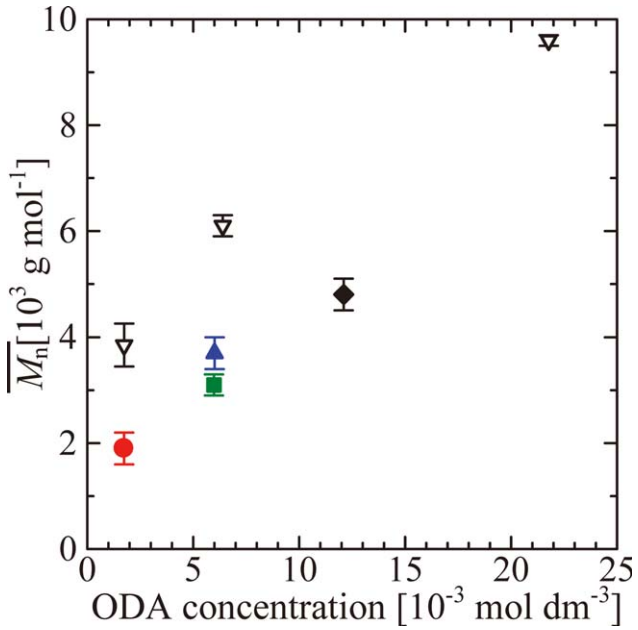

Figure 5. Relationships between ODA concentration and $\overline{M}_n$ of PAA polymerized for 60 min in $scCO_2$ with DMF of 19 mol % at 50°C and in pure DMF at 20°C. Symbols, ●, ▲, ■, ◆: in $scCO_2$ with DMF at 22, 22, 30, and 29 MPa, respectively; ▽ in pure DMF at atmospheric pressure. [Color figure can be viewed in the online issue, which is available at wileyonlinelibrary.com.]

weight average molecular weight ($\overline{M}_w$) of PAA are listed in Table I and in Figures 5 and 6, respectively. The results of the polymerizations of ODA and PMDA in pure DMF at 20°C are also shown in Figures 5 and 6 as the reference data because solution polymerization is the most conventional method. The homogeneous phases were kept during polymerization in pure DMF unlike in $scCO_2$. As shown in Figure 5, the $\overline{M}_n$ of PAA polymerized in $scCO_2$ with 19 mol % DMF increased in an approximate linear fashion as the ODA concentration increased regardless of the differences in pressure. The $\overline{M}_n$ of PAAs obtained in $scCO_2$ with DMF were approximately half compared with those obtained in pure DMF at the same ODA concentration, and the degrees of polymerization estimated based on $\overline{M}_n$ also listed in Table I were not so high even at the highest monomer concentration of the present work. On the other hand, the $\overline{M}_w$ of PAAs obtained in $scCO_2$ with DMF reached a ceiling at about 10^4 g mol^{-1} as described in Table I and Figure 6. These results seemed to have been caused when PAA aggregates were precipitated during polymerization in $scCO_2$, as shown in Figure 3. Therefore, as is the case with the VDP method, the polymerization degree of PAA produced in $scCO_2$ was lower than that produced by the solution polymerization.[29]

The MWD of PAA obtained at an ODA concentration of 5.98×10^{-3} mol dm^{-3} and 30 MPa had an obvious secondary peak in the high molecular weight region as shown in Figure 4, which was the cause of the high polydispersity index for that polymerization condition as listed in Table I. To clarify the difference in the phase behavior based on the difference in pressure, the images of the phase behaviors during polymerization at ODA concentration, about 6.0×10^{-3} mol dm^{-3} and both 22 and 30 MPa, are shown in Figure 7. Most of the PAA aggregates were already precipitated at the bottom of the cell and

Table I. Experimental Results of the Polymerization of API Monomers in $scCO_2$ at 50°C for 60 min

m_{ODA}[a] [10^{-3} mol dm^{-3}]	m_{PMDA}[b]/m_{ODA}	P[c] [MPa]	$\overline{M}_n$ [10^3 g mol^{-1}]	$\overline{M}_w$ [10^3 g mol^{-1}]	$\overline{M}_w/\overline{M}_n$	$\overline{p}_n$[d]
1.74 ± 0.07	1.11 ± 0.02	22 ± 1	1.9 ± 0.3	6.0 ± 1.1	3.2 ± 0.1	4.5 ± 0.9
6.01 ± 0.01	1.10 ± 0.01	22 ± 1	3.7 ± 0.3	8.5 ± 0.3	2.3 ± 0.1	8.8 ± 0.9
5.98 ± 0.15	1.21 ± 0.08	30 ± 1	3.1 ± 0.2	10.8 ± 0.3	3.5 ± 0.2	7.3 ± 0.7
12.1 ± 0.1	1.19 ± 0.01	29 ± 1	4.8 ± 0.3	9.5 ± 0.6	2.0 ± 0.1	11.4 ± 1.2

[a] ODA concentration.
[b] PMDA concentration.
[c] Pressure.
[d] Degree of polymerization.

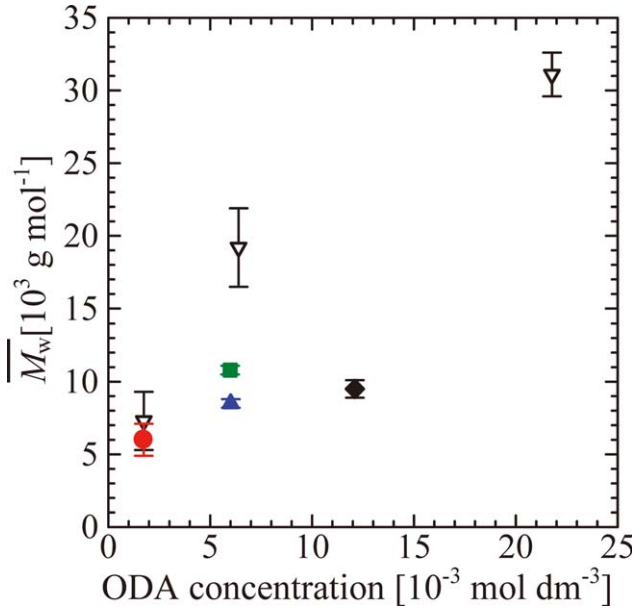

Figure 6. Relationships between ODA concentration and $\overline{M}_w$ of PAA polymerized for 60 min in $scCO_2$ with DMF of 19 mol % at 50°C and in pure DMF at 20°C. Symbols ●, ▲, ■, and ◆ in $scCO_2$ with DMF at 22, 22, 30, and 29 MPa, respectively; ▽ in pure DMF at atmospheric pressure. [Color figure can be viewed in the online issue, which is available at wileyonlinelibrary.com.]

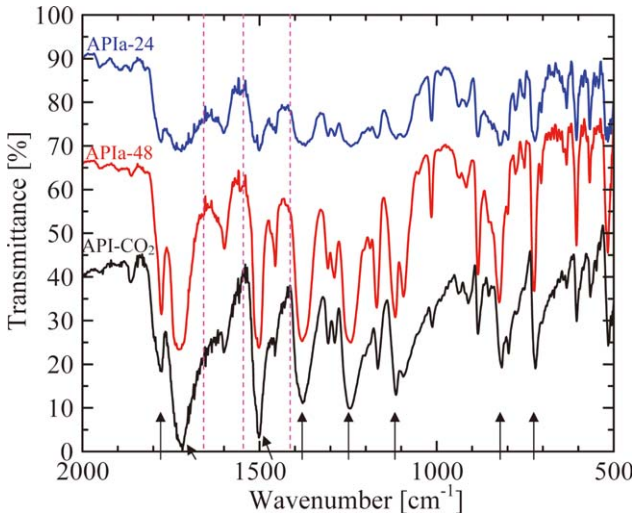

Figure 8. FT-IR spectra of APIs obtained from PAAs synthesized in $scCO_2$ (ODA: 1.21 × 10^{-2} mol dm^{-3}, 29 MPa) and in pure DMF (ODA: 6.40 × 10^{-3}mol dm^{-3}). Spectra, APIa-24 and APIa-48 show APIs obtained from PAAs synthesized in pure DMF then cured at 250°C for 24 and 48 h, respectively, and API-CO_2 represents API obtained from PAA synthesized in $scCO_2$ then cured at 250°C for 24 h. Dashed lines show the wavenumbers indicating vibration modes for the typical functional groups of PAA.[32] [Color figure can be viewed in the online issue, which is available at wileyonlinelibrary.com.]

onto the surface of the windows for 30 min at 22 MPa as shown in the figure. On the other hand, the phase behavior inside the cell was cloudy for 60 min at 30 MPa, and the amount of the PAA aggregates completely precipitated at 30 MPa was smaller than that at 22 MPa despite the same monomer concentration. Therefore, the PAA aggregates were dispersed much better at 30 MPa than at 22 MPa, which is considered to have been because of the increasing solvency power of $scCO_2$ associated with an increase in the density. Moreover, the phase behavior at an ODA concentration of 5.98 × 10^{-3} mol dm^{-3} and 30 MPa showed that the precipitated PAA aggregates were much smaller than those obtained at ODA of 6.01 × 10^{-3} mol dm^{-3} and 22 MPa, and 1.21 × 10^{-2} mol dm^{-3} and 29 MPa, as shown in Figure 3. Therefore, the

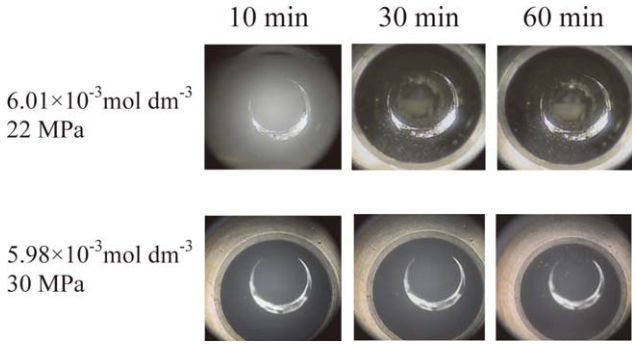

Figure 7. Images of the chronological changes in phase behaviors during polymerization for ODA concentrations of about 6.0 × 10^{-3} mol dm^{-3} at both 22 and 30 MPa. [Color figure can be viewed in the online issue, which is available at wileyonlinelibrary.com.]

portion of PAA that was well dispersed was considered to react better than PAA that was completely precipitated. The results of this study indicated that both the concentration of the monomers and the phase behavior are important factors in the determination of the molecular weight and the MWD of PAA in $scCO_2$. And, the dispersion condition of PAA precipitates changed depending on the monomer concentration and $scCO_2$ density (pressure) at constant temperature.

Next, the FT-IR spectra of APIs obtained from the PAA synthesized both in $scCO_2$ with DMF and in pure DMF are described in Figure 8. The wavenumber was focused between 2000–500 cm^{-1} where many peaks originated from both of the chemical structures of PAA and API.[30–33] In the figure, the spectrum of API obtained from PAA synthesized using 1.21 × 10^{-2} mol dm^{-3} of ODA at 29 MPa in $scCO_2$ with DMF is shown along with the spectra of APIs obtained from PAAs synthesized in pure DMF using 6.40 × 10^{-3} mol dm^{-3} of ODA. The curing duration for imidization was 24 h for PAA of $scCO_2$. On the other hand, the PAAs obtained by the solution polymerization were cured for 24 and 48 h to confirm the effect of curing duration for imidization. Here the APIs prepared by each of the methods are represented as API-CO_2, APIa-24, and APIa-48. Moreover, the dominant peaks attributed to the chemical structure of API and PAA synthesized from ODA and PMDA are summarized in Table II for ease of understanding the figure. As for the comparison of the results of APIa-24 and APIa-48, the wavenumbers of almost all peaks were quite close although the peaks of APIa-24 were small due to the difference in the amount of the API mixed in KBr. Peaks that clearly indicated the imide structure could be found in both spectra at 1718,

Table II. Assignments of the Peaks Obtained by the FT-IR Spectrophotometry for API Obtained from PAA Synthesized in $scCO_2$

Wavenumber (cm^{-1})	Vibrational mode[30–33]
1776	C=O asymmetric stretching
1718	Imide C=O symmetric stretching
1502	C—C stretching (benzene ring)
1378	Imide C—N stretching
1246	Ether C—O—C and anhydride C—O—C stretching
1115	Ether and anhydride C—O—C stretching
816	C—H out-of-plane bending (benzene ring)
721	Imide cyclic C=O bending

1378, and 721 cm^{-1}. On the other hand, the peaks indicating the structure of PAA[32] were hard to find in the spectra at 1664, 1543, and 1415 cm^{-1} resulting from the amide carbonyl stretching, amide N–H bending and the symmetric stretching of the carboxylate ion, respectively. The spectrum of API-CO_2 was quite similar to those of APIa-24 and APIa-48, as shown in the figure. Therefore, the chemical structure of API obtained from PAA synthesized in $scCO_2$ was considered to be similar to that obtained by the imidization of PAA synthesized in pure DMF.

Moreover, the API-CO_2 and APIa-24 were also analyzed by TGA to evaluate the thermal stability. In addition, API obtained from PAA synthesized by the solution polymerization using

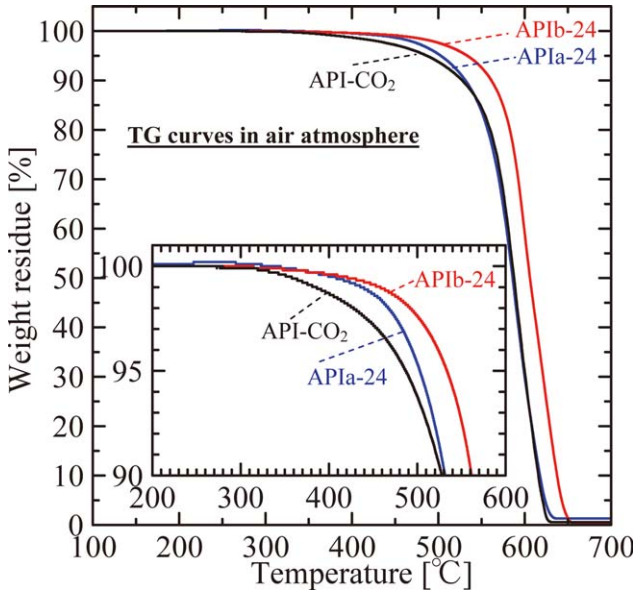

Figure 9. TG curves of APIs obtained from PAAs synthesized in $scCO_2$ (ODA: 1.21 × 10^{-2} mol dm^{-3}, 29 MPa) and in pure DMF (ODA: 6.40 × 10^{-3} and 2.18 × 10^{-2}mol dm^{-3}). Lines: APIa-24 and APIb-24 show APIs obtained from PAAs synthesized in pure DMF at 6.40 × 10^{-3} and 2.18 × 10^{-2}mol dm^{-3} of ODA, respectively, and API-CO_2 represents API obtained from PAA synthesized in $scCO_2$. All PAAs were cured at 250°C for 24 h. Inset shows magnified TG curves more than 90% of weight residue. [Color figure can be viewed in the online issue, which is available at wileyonlinelibrary.com.]

Table III. 5 and 10% Weight Loss Temperatures of APIs Obtained by the TGA Under Air Atmosphere

Sample name	m_{ODA} (10^{-3} mol dm^{-3})	$\overline{M}_n$ (10^3 g mol^{-1})	$\overline{M}_w$ (10^3 g mol^{-1})	$T_{5\%}$ (°C)	$T_{10\%}$ (°C)
API-CO_2	12.1	4.8	9.5	486	528
APIa-24	6.40	6.1	19.2	502	531
APIb-24	21.8	9.6	31.1	534	561

2.18 × 10^{-2} mol dm^{-3} of ODA and cured for 24 h (APIb-24) was also analyzed for investigation of the effect of molecular weight. All measurements were carried out under air atmosphere, and the heating rate was set to 5°C min^{-1}. The results of the TG curves are described in Figure 9, and the temperatures of both 5 and 10% weight loss ($T_{5\%}$ and $T_{10\%}$) obtained are listed in Table III. As for API-CO_2, a remarkable weight loss could not be observed below about 300°C, and the $T_{5\%}$ and $T_{10\%}$ were 486 and 528°C, respectively. The degradation rapidly proceeded from around 500°C, and the weight residue became about zero at 630°C. This behavior was also observed for the measurements of APIa-24 and APIb-24, and was found particularly in TG curves obtained under air atmosphere.[34–36] Both the $T_{5\%}$ and $T_{10\%}$ of API-CO_2 were slightly lower compared with those of APIa-24 and APIb-24, and the order of both the temperatures corresponded to that of the molecular weight. However, the API obtained in $scCO_2$ would be sufficient as polyimide materials in several industrial fields as well as the API obtained from conventional methods. And the properties of API obtained by the $scCO_2$ processing can also be expected to improve much more by operating under more suitable conditions.

In addition, the structural analysis of synthesized PAA using a nuclear magnetic resonator (NMR) should also provide valuable information such as the terminal structure of PAA. On the other hand, sufficient examination of the sample preparation prior to NMR analysis such as solvent exchange from a reaction solvent to a deuterated solvent should be required in order to quantitatively investigate the terminal structure because of the instability of PAA. Therefore, terminal structure analysis using NMR would be an important subject in the future work.

CONCLUSIONS

In this study, the relationships between the polymerization condition, the phase behavior during polymerization, and the molecular weight of PAA were investigated. PAA was polymerized from ODA and PMDA in $scCO_2$ with 19 mol % DMF at 50°C and at several monomer concentrations, and the polymerization pressures were set to about 22 and 30 MPa. The $\overline{M}_n$ of PAA increased with increasing the monomer concentration in the region of ODA concentration from 1.74 × 10^{-3} to 1.21 × 10^{-2} mol dm^{-3} regardless of the difference in pressure. On the other hand, the phase behaviors changed depending on the monomer concentration and $scCO_2$ density, and the $\overline{M}_w$ of PAA depended on the phase behaviors during polymerization

along with monomer concentration. Based on the results of FT-IR spectrophotometry and TG analyses, the chemical structure of API obtained from PAA synthesized in $scCO_2$ was considered to be similar to that obtained by the solution polymerization. Moreover, API obtained from PAA synthesized in $scCO_2$ with 1.21×10^{-2} mol dm^{-3} of ODA at 29 MPa was quite stable to approximately 300°C under an air atmosphere.

ACKNOWLEDGMENTS

This study was supported by Grants-in-Aid for Young Scientists (B) (23760722) from the Ministry of Education, Culture, Science and Technology of Japan and by a research grant from the Kyoto Technoscience Center.

REFERENCES

1. Clair, A. K. S.; Slemp, W. S. *NASA Technical Memorandum* **1985**, 86341.
2. Clair, A. K. S.; Clair, T. L. S.; Slemp, W. S.; Ezzell K. S. *NASA Technical Memorandum* **1985**, 87650.
3. Sroog, C. E. *Prog. Polym. Sci.* **1991**, *16*, 561.
4. Imai, Y.; Yokota, R. Latest Polyimide; NTS Co.: Tokyo, **2002**, pp 1–54 [in Japanese].
5. Naganuma, T.; Naito, K.; Yang, J. M. *Carbon* **2011**, *49*, 3881.
6. Liaw, D. J.; Wang, K. L.; Huang, Y. C.; Lee, K. R.; Lai, J. Y.; Ha, C. S. *Prog. Polym. Sci.* **2012**, *37*, 907–974.
7. Asao, K.; Yoshioka, Y.; Watano, S. *Kagaku Kogaku Ronbunshu* **2012**, *38*, 39.
8. Iijima, M.; Takahashi, Y.; Inagawa, K.; Itoh, A. *J. Vac. Soc. Jpn.* **1985**, *28*, 437.
9. Takahashi, Y.; Iijima, M.; Inagawa, K.; Itoh, A. *J. Vac. Sci. Technol. A* **1987**, *5*, 2253.
10. Salem, J. R.; Sequeda, F. O.; Duran, J.; Lee, W. Y.; Yang, R. M. *J. Vac. Sci. Technol. A* **1986**, *4*, 369.
11. Kuo, C.; Chen, J. J. *Microelectron. Reliab.* **2010**, *50*, 1116.
12. Khor, C. Y.; Abdullah, M. Z.; Ariff, Z. M.; Leong, W. C. *Int. Commun. Heat Mass Transf.* **2012**, *39*, 670.
13. Chen, W. H.; Yu, C. F.; Cheng, H. C.; Tsai, Y.; Lu, S. T. *Microelectron. Reliab.* **2013**, *53*, 30.
14. Long, D. P.; Blackburn, J. M; Watkins, J. J. *Adv. Mater.* **2000**, *12*, 913.
15. Blackburn, J. M.; Long, D. P.; Cabañas, A; Watkins, J. J. *Science* **2001**, *294*, 141.
16. Kondoh, E; Kato, H. *Microelectr. Eng.* **2002**, *64*, 495.
17. Kwon, S; Lee, K.; Bae, W.; Kim, H. *J. Supercrit. Fluids*, **2008**, *45*, 391.
18. Kendall, J. L.; Canelas, D. A.; Young, J. L.; DeSimone, J. M. *Chem. Rev.* **1999**, *99*, 543.
19. Lee, H.; Terry, E.; Zong, M.; Arrowsmith, N.; Perrier, S.; Thurecht, K. J.; Howdle, S. M. *J. Am. Chem. Soc.* **2008**, *130*, 12242.
20. Zetterlund, P. B.; Aldabbagh, F.; Okubo, M. *J. Polym. Sci. Part A* **2009**, *47*, 3711.
21. Chambon, P.; Cloutet, E.; Cramail, H. *Macromolecules* **2004**, *37*, 5856.
22. Said-Galiyev, E. E.; Vygodskii, Y. S.; Nikitin, L. N.; Vinokur, R. A.; Gallyamov, M. O.; Pototskaya, I. V.; Kireev, V. V.; Khokhlov, A. R.; Schaumburg, K. *J. Supercrit. Fluids* **2003**, *26*, 147.
23. Haruki, M.; Fukui, N.; Kobayashi, F.; Kihara, S.; Takishima, S. *Ind. Eng. Chem. Res.* **2011**, *50*, 11942.
24. Haruki, M.; Fukui, N.; Kihara, S.; Takishima, S. *J. Chem. Thermodyn.* **2012**, *54*, 261.
25. Zúñiga-Moreno, A.; Galicia-Luna, L. A. *J. Chem. Eng. Data* **2005**, *50*, 1224.
26. Yang, C. P.; Hsiao, S. H. *J. Appl. Polym. Sci.* **1985**, *30*, 2883.
27. Sugitani, H.; Fukasawa, M.; Uchimura, S. *Hitachi Chem. Tech. Rep.* **1992**, *19*, 675.
28. Duran-Valencia, C.; Valtz, A.; Galicia-Luna, L. A.; Richon, D. *J. Chem. Eng. Data* **2001**, *46*, 1589.
29. Bäte, M.; Neuber, C.; Giesa, R.; Schmidt, H. W. *Macromol. Rapid Commun.* **2004**, *25*, 371.
30. Nishino, T.; Kotera, M.; Inayoshi, N.; Miki, N.; Nakamae, K. *Polymer* **2000**, *41*, 6913.
31. Miyamae, T.; Tsukagoshi, K.; Matsuoka, O.; Yamamoto, S.; Nozoye, H. *Langmuir* **2001**, *17*, 8125.
32. Anthamatten, M.; Letts, S. A.; Day, K.; Cook, R. C.; Gies, A. P; Hamilton, T. P.; Nonidez, W. K. *J. Polym. Sci. A* **2004**, *42*, 5999.
33. González, J. P. P.; Lamure, A.; Senocq, F. *Surf. Coat. Tech.* **2007**, *201*, 9437.
34. Jou, J. H.; Cheng, C. L.; Jou, E. C. Y.; Yang, A. C. M. *J. Polym. Sci. B* **1996**, *34*, 2239.
35. Myung, B. Y.; Kim, J. S.; Kim, J. J.; Yoon, T. H. *J. Polym. Sci. A* **2003**, *41*, 3361.
36. Wang, H.; Paul, D. R.; Chung, T. S. *Polymer* **2013**, *54*, 2324.